

1 **On linking an earth system model to the equilibrium carbon representation of an**  
2 **economically optimizing land use model**

3 Ben Bond-Lamberty<sup>1\*</sup>, Katherine Calvin<sup>1</sup>, Andrew D. Jones<sup>2</sup>, Jiafu Mao<sup>3</sup>, Pralit Patel<sup>1</sup>,  
4 Xiaoying Shi<sup>3</sup>, Allison Thomson<sup>1</sup>, Peter Thornton<sup>3</sup>, and Yuyu Zhou<sup>1</sup>

5  
6 <sup>1</sup>Joint Global Change Research Institute, Pacific Northwest National Laboratory, College  
7 Park, MD, USA

8 <sup>2</sup>Lawrence Berkeley National Laboratory, 1 Cyclotron Rd., MS 74-0171, Berkeley, CA,  
9 USA

10 <sup>3</sup>Environmental Sciences Division, Oak Ridge National Laboratory, Oak Ridge, TN,  
11 USA

12

13 \* Corresponding author: [bondlamberty@pnnl.gov](mailto:bondlamberty@pnnl.gov)

14

15 Submitted to *Geoscientific Model Development*

16 January 26, 2014

17 Revised version submitted June 6, 2014

18 **Final version submitted September 21, 2014**

19

20 **Abstract**

21 Human activities are significantly altering biogeochemical cycles at the global  
22 scale, and the scope of these activities will change with both future climate and  
23 socioeconomic decisions. This poses a significant challenge for earth system models

24 (ESMs), which can incorporate land-use change as **prescribed inputs but do not actively**  
25 **simulate** the policy or economic forces that drive land use change. One option to address  
26 this problem is to couple an ESM with an economically oriented integrated assessment  
27 model, but this is challenging because of the radically different goals and underpinnings  
28 of each type of model. This study describes the development and testing of a coupling  
29 between the terrestrial carbon cycle of an ESM (CESM) and an integrated assessment  
30 (GCAM) model, focusing on how CESM climate effects on the carbon cycle **could** be  
31 shared with GCAM. We examine the best proxy variables to share between the models,  
32 and quantify how carbon flux changes driven by **climate, CO<sub>2</sub> fertilization, and** land-use  
33 changes (e.g. deforestation) can be distinguished from each other by GCAM. The net  
34 primary production and heterotrophic respiration outputs of the Community Land Model  
35 (CLM), the land component of CESM, were found to be the most robust proxy variables  
36 by which to **recalculate** GCAM's assumptions of equilibrium ecosystem steady state  
37 carbon. Carbon-cycle effects of land-use change are spatially limited relative to climate  
38 effects, and thus we were able to distinguish these effects successfully in the model  
39 coupling, passing only the latter to GCAM. This paper does not present results of a fully  
40 coupled simulation but shows, using a series of offline CLM simulations and an  
41 additional idealized Monte Carlo simulation, that our CESM-GCAM proxy variables  
42 reflect the phenomena that we intend, and do not contain erroneous signals due to LUC.  
43 By allowing climate effects from a full ESM to dynamically modulate the economic and  
44 policy decisions of an integrated assessment model, this work will help link these models  
45 in a robust and flexible framework capable of examining two-way interactions between  
46 human and earth system processes.

47

## 48 **1. Introduction**

49 Human activities are significantly altering biogeochemical cycles at the global  
50 scale, e.g. by appropriation of net primary production (Imhoff et al., 2004; Ito, 2011),  
51 modification of natural fire dynamics (Pechony and Shindell, 2010), and fossil fuel  
52 emissions raising atmospheric CO<sub>2</sub> levels (Le Queré et al., 2009). In addition, land-use  
53 change (LUC) exerts strong effects on the global carbon cycle (Bonan, 2008; Caspersen  
54 et al., 2000; Arora and Boer, 2010; Laganière et al., 2009), as well as direct biophysical  
55 effects on albedo and water vapor fluxes, that in turn have significant regional to global  
56 consequences (Brovkin et al., 2013; Jones et al., 2013b). As a result, different policy  
57 choices vis-à-vis LUC and carbon may **result in greatly differences in the future carbon**  
58 **cycle and global climate** (Wise et al., 2009; Jones et al., 2013a), even though the direct  
59 LUC fluxes will likely be far smaller than in the past (Brovkin et al., 2013).

60 This poses a significant challenge for global earth system models (ESMs), in  
61 which fully coupled climate models are used to draw inferences about Earth's past and  
62 future climate states and understand how changes to the radiative properties of Earth's  
63 atmosphere interact with its climate, biogeochemistry, and carbon cycle (Brovkin et al.,  
64 2013; Todd-Brown et al., 2014). Such models may incorporate LUC as **prescribed** inputs,  
65 but do not simulate policy options or economic forces, a significant limitation given how  
66 strongly humans can perturb the earth system (Hurtt et al., 2002; Randerson et al., 2009).  
67 Conversely, integrated assessment models (IAMs) are used to examine the human  
68 components of the Earth system, including greenhouse gas emission sources, and drivers  
69 of land-use change. Their representation of the physical climate and earth system is

70 simplistic, however, with little spatial resolution or process fidelity compared to an ESM  
71 (Meinshausen et al., 2011a; Meinshausen et al., 2011b). These two modeling  
72 paradigms—ESMs with no economic or energy system modeling, and IAMs with only  
73 basic representations of natural processes—developed largely independently of each  
74 other, and their interactions have historically been limited.

75 ESMs and IAMs increasingly need each other’s capabilities, however (van  
76 Vuuren et al., 2012; Houghton, 2013). One solution is to couple an ESM to an IAM,  
77 letting each model specialize in its specific domain while passing information on the  
78 natural and human systems, respectively, between them. This would provide a two-way  
79 coupling within a single integrated system, whereby economic decisions in the IAM  
80 translate directly into trace gas fluxes and land use changes in the ESM, and changes in  
81 the ESM climate feed back onto crop yields, heating and cooling demands, energy  
82 production, etc. in the IAM. Successfully linking such complex, large models would  
83 permit integrated and unprecedented analyses of the interactions between economic  
84 change, climate policy, and the physical earth system, with fully coupled feedbacks  
85 between the economic and physical-science components (van Vuuren et al., 2012).

86 This paper describes the development and testing of a mechanism linking the  
87 terrestrial carbon components of an ESM (CESM, the Community Earth System Model)  
88 with an IAM (the Global Change Assessment Model, GCAM) (**Figure 1**). The goals of  
89 the current study were to develop and test a robust but tractable coupling allowing  
90 GCAM LUC projections to respond to changes in the CESM climate and biogeochemical  
91 cycles. We focus here on the terrestrial aspect of the CESM-to-GCAM coupling, but this

92 is only one component of a larger effort to create a more general integrated Earth System  
93 Model (iESM) (Jones et al., 2013a) as described above.

94

## 95 **2. Materials and Methods**

### 96 *2.1. Model descriptions*

97 Both CESM's Community Land Model (CLM) and GCAM have been extensively  
98 described, and here we note only their most relevant aspects (Gent et al., 2011). The  
99 terrestrial model in the CESM system, CLM simulates the cycling and land-atmosphere  
100 exchange of **energy, water, carbon, and trace gases**. CLM version 4, used in this study,  
101 resulted from merging the biophysical framework of CLM v3.5 (Oleson et al., 2008) with  
102 the carbon and nitrogen dynamics of the biogeochemistry model Biome-BGC (Thornton  
103 et al., 2002; Running and Hunt, 1993). The model incorporates biogeophysics, surface  
104 hydrology, biogeochemistry, and dynamic vegetation components (Bonan et al., 2002),  
105 whose dynamics have been extensively tested (Shi et al., 2011; Oleson et al., 2008;  
106 Lawrence et al., 2008; Mao et al., 2012a; Mao et al., 2012b). Model vegetation is based  
107 on plant functional types (PFTs) occupying dynamic fractions of each grid cell (typically  
108 0.25-2° resolution), with each PFT (1 bare ground, 8 tree, 3 shrub, 3 grass, 1 crop)  
109 characterized by distinct physiological parameters (Oleson et al., 2010). The model's C  
110 and N cycles are closely coupled and include canopy photosynthesis, plant growth and  
111 mortality, photosynthate allocation, and subsurface C and N cycling (Thornton et al.,  
112 2007); at any point in time, CLM tracks a wide suite of above- and belowground C pools  
113 resulting from the integrated effects of these and other (Kloster et al., 2010) processes.

114           The GCAM model, by contrast, is an economic model driven by assumptions  
115 about population size and labor productivity that determine potential gross domestic  
116 product in each of 14 regions; these regions are further divided by GCAM’s agriculture  
117 and land-use submodel into 18 agro-ecological zones or AEZs (Monfreda et al., 2009).  
118 GCAM originated as the energy-economic MiniCAM model (Edmonds and Reilly,  
119 1983), and currently integrates energy, agriculture, forestry, and land markets with a  
120 simple terrestrial carbon cycle (Thomson et al., 2010; Wise et al., 2009). The model  
121 operates on a 5-year timestep, computing simultaneous market-clearing prices for all  
122 energy, agriculture, and land markets (Kim et al., 2006). The model is typically used to  
123 explore the effects of policy scenarios—for example, carbon pricing, emissions  
124 constraints, or capped limits on total radiative forcing (Calvin et al., 2009). Economic  
125 land use decisions **are based** on the relative inherent profitability of using land for  
126 competing purposes. GCAM does not use land use allocation constraints, but its  
127 calibration based on historical data means that history is reflected in future land  
128 allocation decisions (Wise and Calvin, 2010; Wise et al., 2014).

129           GCAM’s **terrestrial** carbon model is fundamentally concerned with calculating  
130 LUC CO<sub>2</sub> emissions resulting from the model’s economic decisions. It does this by  
131 determining the C stocks changes with every land use change, and allocating those as C  
132 fluxes over time. Specifically, each land use (**i.e., the model’s various crops, forest types,**  
133 **etc.**, in each AEZ of each political region) has above- (vegetation) and belowground  
134 (soil) steady-state C densities associated with it, values currently based on Houghton  
135 (1999). These values vary by AEZ and political region and do not change during the  
136 model run; i.e., land is assumed to be in C equilibrium with the atmosphere in the

137 absence of LUC. When a particular land-use **category** contracts in area, all the lost  
138 aboveground C (i.e. the land-use's C density multiplied by the change in area) is emitted  
139 instantaneously, while its belowground C is emitted in an exponential decay pattern.  
140 When a land-use **category** expands, the resulting C uptake depends on the length of time  
141 it takes for the vegetation to mature (from 1 yr for crops to 30-100 yr for forests),  
142 following a Bertalanffy-Richards growth function. Carbon emission and sequestration  
143 thus result only from changes in land use, with emission from shrinking land-use  
144 **categories** set against uptake from growing ones. The model computes these fluxes across  
145 time but, importantly, does not track current C stocks in the manner of CLM or most land  
146 surface models. Further details on the agriculture, land use, and carbon cycle assumptions  
147 and algorithms of GCAM may be found in its online documentation  
148 (<http://wiki.umd.edu/gcam>) and several publications (Wise et al., 2014; Wise and Calvin,  
149 2010).

150 In the iESM architecture a third model, the Global Land Model or GLM  
151 ([http://eos-webster.sr.unh.edu/data\\_guides/glm\\_dg.jsp](http://eos-webster.sr.unh.edu/data_guides/glm_dg.jsp)), currently downscales GCAM's  
152 land use decisions (made on agro-ecological zones at the regional level) onto CLM's  
153 global grid (**Figure 1**). This step uses algorithms and assumptions described by Di  
154 Vittorio et al. (2014) and Lawrence et al. (2012), and is not detailed further here, as this  
155 study focuses only on the coupling from CLM to GCAM.

156

## 157 *2.2. Issues in linking the CLM and GCAM carbon cycles*

158 The fundamental conceptual, as opposed to technical, problem in linking the  
159 CLM and GCAM carbon cycle models is that the former tracks time-varying C pools and

160 fluxes, while the latter bases its economic optimization on long-term (equilibrium) C  
161 pools for large regions, and only computes LUC fluxes. Replacing GCAM’s entire  
162 internal carbon cycle (and its reliance on equilibrium C) may be possible in the long term,  
163 but would require a fundamental rewriting of this complex model’s agriculture and land-  
164 use code. In this study a looser coupling between CLM and GCAM was deemed more  
165 tractable, while also sufficient for the experiments described here. Such an approach  
166 transmits relative changes between the models while allowing baseline data, against  
167 which the models have been calibrated and tested, to differ.

168         Such a ‘loose’ coupling means that when a CLM grid cell’s carbon cycle changes,  
169 we need to (i) have a suitable proxy by which to change **the values of** GCAM’s steady-  
170 state carbon assumptions, and (ii) distinguish LUC effects on carbon fluxes from climate  
171 and other (CO<sub>2</sub>, N deposition, etc.) effects, because only the latter should affect GCAM’s  
172 assumptions of equilibrium C stocks. For example, **if the land carbon pool size of a grid**  
173 **cell with forested fraction simulated by CLM changes** from one time step to the next  
174 because of harvest, this should not affect GCAM’s economic optimization—the forest  
175 will regrow to the same equilibrium state. If the same forest’s carbon pool rises because  
176 of CO<sub>2</sub> fertilization, however, this information (i.e., there is more C sequestration  
177 potential available for this land use type) needs to be propagated to GCAM’s assumptions  
178 about long-term pool potentials. Distinguishing these sources is thus critical (Gasser and  
179 Ciais, 2013).

180

181 *2.3. Identifying the best proxy variables to link CLM to GCAM*



182           Given the decision to adjust GCAM’s equilibrium C assumptions based on  
183 relative changes in the CLM carbon cycle, one possible proxy variable to pass between  
184 the models was CLM’s time-varying carbon pools, based on the assumption that short-  
185 term pool changes will translate to longer-term (i.e. equilibrium, as needed by GCAM)  
186 storage changes. These data may be more vulnerable to LUC effects than carbon flux  
187 data, however, as fluxes typically recover much faster from disturbance than do the  
188 slower pools (Amiro et al., 2010; Goetz et al., 2012). Short-term changes in C fluxes can  
189 be analytically related to steady-state C pools in models, even in the presence of  
190 ecosystem disturbances (Hurtt et al., 2010). This needed to be tested and demonstrated  
191 for CLM, however.

192           We tested potential proxy variables in two ways. First, we ran a series of single  
193 forcing factor experiments in CLM, looking at how changes in each factor affected CLM  
194 carbon stocks and fluxes (specifically, gross primary production, net primary production  
195 or NPP, heterotrophic respiration or HR, soil organic matter, vegetation carbon, and total  
196 ecosystem carbon). The three forcing factors tested were atmospheric CO<sub>2</sub>, as alleviating  
197 the CO<sub>2</sub> constraints on leaf-level photosynthesis may cascade up to ecosystem carbon  
198 storage (Gedalof and Berg, 2010; Lenton and Huntingford, 2003); nitrogen deposition, a  
199 potentially strong constraint on the current and future global carbon cycle (Galloway et  
200 al., 2005; Norby et al., 2010); and LUC, which affects both immediate and long-term  
201 land-atmosphere interactions (Caspersen et al., 2000; Pongratz et al., 2009). A ‘good’  
202 proxy variable would be strongly affected by the first two, CO<sub>2</sub> and N, but not by LUC  
203 (as only the former two will affect equilibrium C; see above), and would accurately  
204 reflect climate-driven changes to equilibrium C stocks in CLM.

205 In simulation S1 (the control), we used 1901-1920 climate drivers for the entire  
206 period 1850-2010, and kept atmospheric CO<sub>2</sub> concentration, nitrogen deposition, and  
207 land cover constant at their 1850 values. In transient 1850-2010 simulations S2-S4, we  
208 used the same looped 1902-1920 climate, and varied one of the three factors in each  
209 while holding the other two factors constant (**Table 1**). The time varying factors were  
210 based on transient datasets constructed to mimic as closely as possible the historical  
211 record over the period 1850-2010, as described by Shi et al. (2013). The effect of each  
212 individual factor was then calculated by subtracting S1 from simulations S2, S3 and S4.  
213 The CRUNCEP data used to drive these uncoupled simulations is a combination of the  
214 CRU TS.2.1 0.5° monthly 1901-2002 climatology (Mitchell and Jones, 2005) and the  
215 2.5° NCEP2 reanalysis data beginning in 1948 and available in near real time (Kanamitsu  
216 et al., 2002; Mao et al., 2012b).

217 Second, we examined how well NPP in particular was related to equilibrium C  
218 stocks in CLM only (i.e. before any coupling to GCAM). This involved two offline  
219 experiments (**Table 1**) with a repeating 5-year climate drawn either from the beginning  
220 (2005-2009, simulation E1) or end (2090-2094, simulation E2) of an RCP4.5 coupled  
221 simulation (Taylor et al., 2012). We quantified how well (i) NPP in the first 5 years of  
222 simulation E1 predicted total vegetation C in the final 5 years, and (ii) the change in NPP  
223 resulting from an altered climate state (E2 minus E1) predicted the relative change in C  
224 pools over the final years of the two simulations.

225 Taken together, these experiments tested how well NPP could be used to predict  
226 equilibrium C under both constant and changing climate. The state of the terrestrial  
227 carbon system at the beginning of these simulations reflected the disturbance and climate

228 histories of the 20<sup>th</sup> century, with various different non-equilibrium C states across  
229 different grid cells and PFTs. Land cover was fixed at 2000 values, and we ran the E1  
230 and E2 simulations for 150 model years with no additional LUC in order to allow the  
231 carbon stocks to approach their equilibrium state. It is important to note that we did not  
232 disable the fire algorithms in CLM. Fire significantly influences model stocks and fluxes  
233 (Li et al., 2014), and thus rather than converging to a single steady-state carbon stock,  
234 PFTs influenced by fire converged to a quasi-equilibrium characterized by periodic  
235 carbon losses due to fire followed by periods of recovery.

236

#### 237 *2.4. Distinguishing climate from land-use signals*

238 As noted above, it is important to distinguish carbon cycle changes caused by  
239 LUC, versus those caused by climate change. For the CLM to GCAM coupling, even a  
240 perfect proxy variable will be subject to **climate and land-use changes** during a CESM  
241 run, both before the run starts (i.e., during spinup or initialization phases) as well as  
242 during a model run. For example, a cell in which a new PFT is established immediately  
243 prior to an iESM run would have very low C stocks and NPP in the first timestep; as its  
244 vegetation regrows, the cell would appear, to GCAM, to be undergoing enormous  
245 productivity increases. Conversely, significant expansion of a PFT (e.g., agriculture  
246 reverting to forest) during the iESM run might appear to have drastically lowered  
247 productivity, leading GCAM to redirect land away from that PFT. Both of these cases  
248 cause problems for GCAM because productivity drives decision-making in the model,  
249 which bases its land-use decisions based on the relative inherent profitability of using

250 land for competing purposes (Wise and Calvin, 2010). As a result apparent changes in  
251 productivity produce changes in profit (as measured in U.S. dollars) and thus land use.

252 Thus in both cases, we need to exclude cells with anomalously large C changes,  
253 driven by LUC, from the final numeric scalars (i.e., the proxy variables signaling how  
254 much GCAM should adjust its assumptions of equilibrium C) computation. They will  
255 bias the computation of the scalars, and lead GCAM into a possible feedback loop: if the  
256 model sees highly anomalous values, it may allocate more land to those PFTs, resulting  
257 in higher profits and further land use change in the region with the anomaly. (A negative  
258 feedback is also possible; both cases occur because the changed productivity alters the  
259 relative profitability of the different land uses, and profit maximization is the  
260 fundamental decision-making criterion in GCAM.)

261 To distinguish the effect of LUC (as opposed to climate effects) on primary CO<sub>2</sub>  
262 fluxes and land carbon pools, we assumed that climate change will have a broad spatial  
263 distribution, either global or regional, while LUC will affect relatively small groups of  
264 cells in any particular timestep; this obviously may not hold in particular regions and  
265 points in time (Arora and Boer, 2010), but should be broadly true across the millions of  
266 data points ( $\sim 10^5$  grid cells x PFT combinations) being output by CLM. Thus a statistical  
267 outlier test, comparing how much any particular cell's carbon cycle has changed relative  
268 to the start of the run, should be able to exclude cells whose inferred change in long-term  
269 carbon density fall significantly outside of the norm. To do so we used a method based on  
270 median absolute deviation (Davies and Gather, 1993), a robust (insensitive to outliers)  
271 measure of central tendency. The scalars were then mapped from CLM's PFTs and grid

272 cells to GCAM's land-cover types and AEZ regions, weighted by PFT area, land area in  
273 each grid cell, and cell area in the AEZ.

274 This technique depends on the overall population mean not being overly  
275 perturbed, and thus will not work in extreme scenarios of mass deforestation (e.g., Bonan  
276 et al., 1992). An important question is how soon, under increasing amounts of LUC, bias  
277 (i.e., LUC effects masquerading as climate change to GCAM) will be introduced into the  
278 iESM model system. We used a Monte Carlo simulation (M1 in **Table 1**), written in the  
279 statistical package R 2.15.1 (R Development Core Team, 2012), to examine how robust  
280 this outlier exclusion method would be to different levels of LUC, and what if any bias it  
281 might introduce to the GCAM carbon density values. For this exercise, 10,000 cells (**with**  
282 **normalized, unitless data**) were simulated in which a constant +10% climate-change  
283 effect on equilibrium C was presumed to be occurring (Jain and Yang, 2005). A LUC  
284 effect, ranging from -500% to +500% and affecting from 5% to 95% of the cells, was  
285 then additionally applied. The outlier exclusion test defined above was then calculated on  
286 the cells, and a putative signal calculated on the remaining cells. **This inferred climate**  
287 **change was then compared to the original known climate signal to estimate how much**  
288 **error (i.e., the difference between the two signals) would be introduced into iESM under**  
289 **such circumstances.**

290

### 291 **3. Results and Discussion**

#### 292 *3.1. Single-forcing tests: identifying the best proxy variables*

293 Clear differences emerged between the potential proxy variables tested in CLM in  
294 response to three different forcing factors (**Figure 2**). Most notably, carbon stocks were

295 much more sensitive to LUC than were carbon fluxes. This result matches both theory  
296 (Odum, 1969) and a wide variety of field studies (Amiro et al., 2010; Goetz et al., 2012):  
297 stocks are by their nature integrative and accumulate relatively slowly compared to C  
298 flux changes. In contrast, the C flux variables were highly sensitive to climate effects, but  
299 exhibited low sensitivity to LUC.

300 A second, related problem arising from the use of carbon stocks as proxy  
301 variables can be seen in **Figure 3**. In this case a test coupling between CLM and GCAM,  
302 using carbon stocks to pass climate-change information, produced sharp and unrealistic  
303 changes from the GCAM RCP4.5 control run. (This occurred even when running the  
304 outlier-exclusion protocol described above.) Global LUC emissions climbed throughout  
305 the 21<sup>st</sup> century in a departure from the RCP4.5 control, because a few CLM grid cells,  
306 located in GCAM's "Middle East" region, were subject to LUC at the end of CLM's  
307 **transient simulation** phase. As a result, their C stocks (and GCAM's estimation of their  
308 long-term potential C) increased rapidly in the early years of the model run, leading  
309 GCAM to pour more resources into these cells (because these cells' productivity  
310 appeared extraordinarily high, as described in the Methods). Increasing the area of newly  
311 planted bioenergy crops created an even stronger signal of rapidly increasing carbon  
312 stocks, exacerbating the original problem and causing GCAM to put even more resources  
313 into the region. By the end of the century, GCAM was mistakenly growing a huge  
314 percentage of the world's bioenergy crops in the region, on a very small area of land  
315 (**Figure 3**). Conversely, the use of NPP and HR caused no such problems, because of  
316 their relatively fast recovery from LUC disturbance (**cf. Figure 2**).

317 The two primary fluxes determining carbon balance (net primary production and  
318 heterotrophic respiration, NPP and HR) were thus chosen as proxy variables linking  
319 CLM to GCAM, with CLM NPP changes used to scale GCAM's assumptions of  
320 aboveground equilibrium C, while a combination of NPP and HR provided a relative  
321 scaling for GCAM's belowground carbon, **computed at 5-year coupling step as:**

$$C_A = C_{A0} \frac{NPP}{NPP_0} \quad (1)$$

$$C_B = C_{B0} \left[ \frac{NPP}{NPP_0} + \frac{HR_0}{HR} \right] / 2 \quad (2)$$

322 Here the ratio of **NPP (at the current time step) to NPP** at the beginning of the run ( $NPP_0$ )  
323 determines how aboveground equilibrium C in GCAM ( $C_A$ ) **will change relative to the**  
324 **beginning of the run ( $C_{A0}$ ).** CLM's NPP and HR together determine changes in GCAM  
325 equilibrium belowground carbon ( $C_B$ ); note that as NPP and HR get larger/smaller and  
326 smaller/larger compared to their starting values, GCAM's equilibrium C rises/falls.

327

### 328 3.2. Correlation between NPP and equilibrium pools in CLM

329 Simulations E1 and E2 provided insight into the relationship between NPP and  
330 equilibrium C pools within CLM. NPP at the beginning of the E1 simulation was a good  
331 predictor of the equilibrium pools values at the end of the simulation (**Figure 4**), although  
332 the slope of this relationship varied for different PFTs. It was also apparent that this  
333 relationship breaks down at very low NPP values for some PFTs. This result is consistent  
334 with ecological theory and observations, as freshly disturbed ecosystems require a period  
335 of initial growth before NPP stabilizes. These very low NPP values were reliably  
336 excluded by the outlier exclusion method discussed above and tested below.

337 We also found that the change in NPP resulting from an altered pattern of climate  
338 (comparing simulations E1 and E2) was a relatively good predictor of the subsequent  
339 change in equilibrium C stocks. **Table 2** shows the slopes of the linear relationships  
340 between the change in initial NPP (simulation E2 minus E1) and change in equilibrium C  
341 for each PFT in CLM. The initial (2005-2009) change in NPP was able to explain 19-  
342 92% of the variance in the C pool change over the 21<sup>st</sup> century simulation with one  
343 exception (broadleaf evergreen shrubs, 6%). In general, NPP was a better predictor for  
344 relatively high-carbon forest ecosystems, as compared to grasses, shrubs, and crops. This  
345 is good, as high-C systems are particularly important for GCAM: changes in their land  
346 areas exert disproportionate effects on atmospheric CO<sub>2</sub>, which the model is frequently  
347 trying to minimize.

348 To determine whether fire dynamics were responsible for some of the  
349 unexplained variance in equilibrium C pools, we performed the same analysis a second  
350 time, excluding PFT-gridcell combinations in which the cumulative carbon loss from fire  
351 over the 150 year E1 simulation exceeded 800 g C m<sup>-2</sup>. This led to moderate (generally 5-  
352 10%) improvements in the R<sup>2</sup> values in all PFTs except the two broadleaf evergreen  
353 PFTs, and moderate increases in the regression slopes, indicating that fire-influenced  
354 regions tend to have lower C values than others. This is consistent with both observations  
355 and CLM's general fire characteristics (Li et al., 2014), and suggests that fire dynamics  
356 and fire regime changes in response to climate change are important to account for when  
357 constructing simple proxies that can predict changes in future terrestrial carbon stocks  
358 based on evolving climatic and ecological conditions.  
359



360 *3.3. Distinguishing the effects of LUC from climate*

361 The initial experiments thus established the best available variables to loosely  
362 couple CESM and GCAM. But how well could the coupling—specifically, statistically  
363 excluding CLM grid cells whose carbon fluxes were changing ‘too fast’—separate LUC  
364 and climate signals? The M1 experiment results (**Figure 5**) suggested that as long as  
365 fewer than ~25% of the simulation cells were **disturbed**, the error (between the known  
366 climate signal and that inferred by the outlier test) remained **relatively small (<20%)**.  
367 Even when larger numbers of cells were perturbed, the LUC effect had to be quite large  
368 to exceed this level. Because the outlier test is applied to the global population, and not  
369 sub-regions, this implies that only under extreme scenarios will this mechanism start to  
370 introduce substantial error. (In test iESM runs attempting to reproduce RCP 4.5, 4-8% of  
371 the global grid cells were excluded—i.e., failed the outlier test—at each timestep.)

372

373 *3.4. Implications of the loose coupling between CLM and GCAM*

374 For the initial construction of the iESM system, we chose a ‘loose’ coupling  
375 between the ESM and IAM, in which GCAM’s equilibrium C assumptions of various  
376 ecosystems tracked the *relative* changes in CLM’s short-term C fluxes, after exclusion of  
377 LUC effects. This has the advantage of not requiring a fundamental rewriting of GCAM,  
378 as the mathematical formulae and economic principles underlying its land-use decisions  
379 are based on equilibrium C (Wise and Calvin, 2010). In addition, it guarantees that if  
380 climate **change affects** the carbon cycle, GCAM’s equilibrium assumptions will change  
381 correspondingly for the same vegetation type and spatial location, **feeding back into**  
382 **economic and land-use decisions that propagate back to CLM** (Di Vittorio et al., 2014).

383           This is a powerful improvement over the fixed assumptions of both IAMs and  
384 ESMS in these areas, sidestepping the lack of process fidelity and spatial resolution (for  
385 the IAM) and addressing the lack of human agency (for the ESM). The loose coupling  
386 does have disadvantages, however, requiring the statistical identification of outlier grid  
387 cells and inevitable mismatches between the models' definitions of PFTs, C pools, and  
388 time steps (Di Vittorio et al., 2014). In addition, the outlier-exclusion step will break  
389 down under extreme LUC scenarios, **scenarios that while unrealistic can be a useful**  
390 **research tool** (Bonan, 2008; Nobre et al., 1991; Thomson et al., 2010). **This is a particular**  
391 **concern given that the current mechanism was only tested under the relatively moderate**  
392 **RCP 4.5**. For these reasons, we anticipate that the long-term solution is a full  
393 incorporation of an IAM into an ESM, with a unified C cycle.

394

#### 395 **4. Conclusions**

396           Here we have implemented and tested a coupling mechanism between the carbon  
397 cycles of an earth system model (CLM) and an integrated assessment (GCAM) model.  
398 CLM's net primary production and heterotrophic respiration outputs were found to be the  
399 most robust proxy variables by which to manipulate GCAM's assumptions of long-term  
400 ecosystem steady state carbon, with short-term forest NPP shifts strongly correlated with  
401 long-term biomass changes in particular. By assuming the carbon cycle effects of land-  
402 use change are short-term and spatially limited relative to widely distributed climate  
403 effects, we were able to distinguish these effects successfully in the model coupling,  
404 passing only the latter to GCAM. Increasingly extreme LUC scenarios will eventually  
405 break down this mechanism, however.

406           This work is only one step to a full coupling of an ESM and IAM; the second is  
407 described by Di Vittorio et al. (Di Vittorio et al., 2014), and consists of land-use and  
408 land-cover harmonization steps that allow CLM to achieve higher afforestation and wood  
409 harvest rates than possible in the CMIP5 process. By allowing climate effects on the  
410 CLM carbon cycle to modulate, in real time, the economic and policy decisions of an  
411 integrated assessment model, it provides a foundation for further development of the  
412 iESM project linking these models in a robust and flexible framework. Such a framework  
413 will, in turn, facilitate future modeling of the two-way interactions between human and  
414 earth system processes.

415

#### 416 **Acknowledgements**

417           We are grateful to the DOE Office of Science Integrated Assessment Research  
418 Program and Earth System Modeling Program for funding through the integrated Earth  
419 System Modeling Project. This research used resources of the National Energy Research  
420 Scientific Computing Center, which is supported by the Office of Science of the U.S.  
421 Department of Energy under Contract DE-AC02-05CH11231. The CESM project is sup-  
422 ported by the National Science Foundation and the Office of Science (Biological and  
423 Environmental Research) of the U.S. Department of Energy. We thank S. Smith for his  
424 thoughtful comments on an early draft.

425

#### 426 **References**

427 Amiro, B. D., Barr, A. G., Barr, J. G., Black, T. A., Bracho, R., Brown, M., Chen, J. M.,  
428 Clark, K. L., Davis, K. J., Desai, A. R., Dore, S., Engel, V., Fuentes, J. D.,

429 Goldstein, A. H., Goulden, M. L., Kolb, T. E., Lavigne, M. B., Law, B. E.,  
430 Margolis, H. A., Martin, T. A., McCaughey, J. H., Misson, L., Montes-Helu, M.  
431 C., Noormets, A., Randerson, J. T., Starr, G., and Xiao, J.: Ecosystem carbon  
432 dioxide fluxes after disturbance in forests of North America, *J. Geophys. Res.-*  
433 *Biogeosci.*, 115, G00K02, [10.1029/2010JG001390](https://doi.org/10.1029/2010JG001390), 2010.

434 Arora, V., and Boer, G. J.: Uncertainties in the 20th century carbon budget associated  
435 with land use change, *Global Change Biol.*, 16, 3327-3348, [10.1111/j.1365-](https://doi.org/10.1111/j.1365-2486.2010.02202.x)  
436 [2486.2010.02202.x](https://doi.org/10.1111/j.1365-2486.2010.02202.x), 2010.

437 Bonan, G. B., Pollard, D., and Thompson, S. L.: Effects of boreal forest vegetation on  
438 global climate, *Nature*, 359, 716-718, 1992.

439 Bonan, G. B., Oleson, K. W., Vertenstein, M., Levis, S., Zeng, X. B., Dai, Y., Dickinson,  
440 R. E., and Yang, Z.-L.: The land surface climatology of the community land  
441 model coupled to the NCAR community climate model, *J. Climate*, 15, 3123-  
442 3149, 2002.

443 Bonan, G. B.: Forests and climate change: forcings, feedbacks, and the climate benefits  
444 of forests, *Science*, 320, 1444-1449, [10.1126/science.1155121](https://doi.org/10.1126/science.1155121), 2008.

445 Brovkin, V., Boysen, L., Arora, V., Boisier, J. P., Cadule, P., Chini, L., Claussen, M.,  
446 Friedlingstein, P., Gayler, V., van den Hurk, B. J. J. M., Hurtt, G. C., Jones, C. D.,  
447 Kato, E., de Noblet-Ducoudré, N., Pacifico, F., Pongratz, J., and Weiss, M. S.:  
448 Effect of anthropogenic land-use and land-cover changes on climate and land  
449 carbon storage in CMIP5 projections for the twenty-first century, *J. Climate*, 26,  
450 6859-6881, [10.1175/JCLI-D-12-00623.1](https://doi.org/10.1175/JCLI-D-12-00623.1), 2013.

451 Calvin, K. V., Edmonds, J. A., Bond-Lamberty, B., Clarke, L. E., Kim, S. H., Kyle, G. P.,

452 Smith, S. J., Thomson, A. M., and Wise, M.: 2.6: Limiting climate change to 450  
453 ppm CO<sub>2</sub> equivalent in the 21st century, *Energy Economics*, 31, S107-S120,  
454 [10.1016/j.eneco.2009.06.006](https://doi.org/10.1016/j.eneco.2009.06.006), 2009.

455 Caspersen, J. P., Pacala, S. W., Jenkins, J. C., Hurtt, G. C., Moorcroft, P. R., and Birdsey,  
456 R. A.: Contributions of land-use history to carbon accumulation in U.S. forests,  
457 *Science*, 290, 1148-1151, [10.1126/science.290.5494.1148](https://doi.org/10.1126/science.290.5494.1148), 2000.

458 Davies, L., and Gather, U.: The identification of multiple outliers, *Journal of the*  
459 *American Statistical Association*, 88, 782-792, 1993.

460 Di Vittorio, A. V., Chini, L., Bond-Lamberty, B., Mao, J., Shi, X., Truesdale, J.,  
461 Branstetter, M. L., Collins, W. D., Thornton, P. E., Edmonds, J. A., Thomson, A.  
462 M., Hurtt, G. C., Calvin, K. V., Jones, A. D., and Craig, T.: From land use to land  
463 cover: Restoring the afforestation signal in GCAM to CESM land coupling and  
464 the implications for CMIP5 RCP simulations, *Biogeosciences*, in prep, 2014.

465 Edmonds, J. A., and Reilly, J.: A long-term global energy-economic model of carbon  
466 dioxide release from fossil fuel use, *Energy Economics*, 5, 74-88, 1983.

467 Galloway, J. N., Townsend, A. R., Erisman, J. W., Bekunda, M., Cai, Z., Freney, J. R.,  
468 Martinelli, L. A., Seitzinger, S. P., and Sutton, M. A.: Transformation of the  
469 nitrogen cycle: recent trends, questions, and potential solutions, *Science*, 320,  
470 889-892, [10.1126/science.1136674](https://doi.org/10.1126/science.1136674), 2005.

471 Gasser, T., and Ciais, P.: A theoretical framework for the net land-to-atmosphere CO<sub>2</sub>  
472 flux and its implications in the definition of "emissions from land-use change",  
473 *Earth System Dynamics Discussions*, 4, 179-217, [10.5194/esdd-4-179-2013](https://doi.org/10.5194/esdd-4-179-2013),  
474 2013.

475 Gedalof, Z. e., and Berg, A. A.: Tree ring evidence for limited direct CO<sub>2</sub> fertilization of  
476 forests over the 20th century, *Glob. Biogeochem. Cycles*, 24, GB3027,  
477 10.1029/2009GB003699, 2010.

478 Gent, P. R., Danabasoglu, G., Donner, L. J., Holland, M. M., Hunke, E. C., Jayne, S. R.,  
479 Lawrence, D. M., Neale, R. B., Rasch, P. J., Vertenstein, M., Worley, P. H.,  
480 Yang, Z.-L., and Zhang, M.: The Community Climate System Model Version 4, *J.*  
481 *Climate*, 24, 4973-4991, 10.1175/2011JCLI4083.1, 2011.

482 Goetz, S. J., Bond-Lamberty, B., Harmon, M. E., Hicke, J. A., Houghton, R. A.,  
483 Kasischke, E. S., Law, B. E., McNulty, S. G., Meddens, A. J. H., Mildrexler, D.,  
484 O'Halloran, T. L., and Pfeifer, E. M.: Observations and assessment of forest  
485 carbon recovery following disturbance in North America, *J. Geophys. Res.-*  
486 *Biogeosci.*, 117, G02022, 10.1029/2011JG001733, 2012.

487 Houghton, R. A.: The annual net flux of carbon to the atmosphere from changes in land  
488 use 1850–1990, *Tellus*, 51, 298-313, [10.1034/j.1600-0889.1999.00013.x](https://doi.org/10.1034/j.1600-0889.1999.00013.x), 1999.

489 Houghton, R. A.: Keeping management effects separate from environmental effects in  
490 terrestrial carbon accounting, *Global Change Biol.*, 19, 2609-2612,  
491 10.1111/gcb.12233, 2013.

492 Hurtt, G. C., Pacala, S. W., Moorcroft, P. R., Caspersen, J. P., Shevliakova, E.,  
493 Houghton, R. A., and Moore III, B.: Projecting the future of the U.S. carbon sink,  
494 *Proc. Nat. Acad. Sci.*, 99, 1389-1394, 10.1073/pnas.012249999, 2002.

495 Hurtt, G. C., Fisk, J. P., Thomas, R. Q., Dubayah, R. O., Moorcroft, P. R., and Shugart,  
496 H. H.: Linking models and data on vegetation structure, *J. Geophys. Res.-*  
497 *Biogeosci.*, 115, G00E10, [10.1029/2009JG000937](https://doi.org/10.1029/2009JG000937), 2010.

498 Imhoff, M. L., Bouana, L., Ricketts, T., Loucks, C., Harriss, R. C., and Lawrence, W. T.:  
499 Global patterns in human consumption of net primary production, *Nature*, 429,  
500 870-873, 10.1038/nature02619, 2004.

501 Ito, A.: A historical meta-analysis of global terrestrial net primary productivity: Are  
502 estimates converging?, *Global Change Biol.*, 17, 3161-3175, 10.1111/j.1365-  
503 2486.2011.02450.x, 2011.

504 Jain, A. K., and Yang, X.: Modeling the effects of two different land cover change data  
505 sets on the carbon stocks of plants and soils in concert with CO<sub>2</sub> and climate  
506 change, *Glob. Biogeochem. Cycles*, 19, GB2015, 10.1029/2004GB002349, 2005.

507 Jones, A. D., Collins, W. D., Edmonds, J. A., Torn, M. S., Janetos, A. C., Calvin, K. V.,  
508 Thomson, A. M., Chini, L., Mao, J., Shi, X., Thornton, P. E., Hurtt, G. C., and  
509 Wise, M.: Greenhouse gas policies influence climate via direct effects of land use  
510 change, *J. Climate*, 26, 3657-3670, 10.1175/JCLI-D-12-00377.1, 2013a.

511 Jones, A. D., Collins, W. D., and Torn, M. S.: On the additivity of radiative forcing  
512 between land use change and greenhouse gases, *Geophys. Res. Lett.*, 40, 4036-  
513 4041, 10.1002/grl.50754, 2013b.

514 Kanamitsu, M., Ebisuzaki, W., Woollen, J., Yang, S.-K., Hnilo, J. J., Fiorino, M., and  
515 Potter, G. L.: NCEP–DOE AMIP-II Reanalysis (R-2), *Bulletin of the American*  
516 *Meteorological Society*, 83, 1631-1643, 10.1175/BAMS-83-11-1631, 2002.

517 Kim, S. H., Edmonds, J. A., Lurz, J., Smith, S. J., and Wise, M.: The O<sup>bj</sup>ECTS  
518 framework for integrated assessment: Hybrid modeling of transportation, *Energy*  
519 *Journal*, 27, 63-91, 2006.

520 Kloster, S., Nahowald, N. M., Randerson, J. T., Thornton, P. E., Hoffman, F. M., Levis,

521 S., Lawrence, P. J., Feddema, J. J., Oleson, K. W., and Lawrence, D. M.: Fire  
522 dynamics during the 20th century simulated by the Community Land Model,  
523 *Biogeosciences*, 7, 1877-1902, [10.5194/bg-7-1877-2010](https://doi.org/10.5194/bg-7-1877-2010), 2010.

524 Laganière, J., Angers, D. A., and Paré, D.: Carbon accumulation in agricultural soils after  
525 afforestation: a meta-analysis, *Global Change Biol.*, 16, 439-453, [10.1111/j.1365-](https://doi.org/10.1111/j.1365-2486.2009.01930.x)  
526 [2486.2009.01930.x](https://doi.org/10.1111/j.1365-2486.2009.01930.x), 2009.

527 Lawrence, D. M., Slater, A. G., Romanovsky, V. E., and Nicolsky, D. J.: Sensitivity of a  
528 model projection of near-surface permafrost degradation to soil column depth and  
529 representation of soil organic matter, *J. Geophys. Res.*, 113, F02011,  
530 [10.1029/2007jf000883](https://doi.org/10.1029/2007jf000883), 2008.

531 Lawrence, P. J., Feddema, J. J., Bonan, G. B., Meehl, G. A., O'Neill, B. C., Oleson, K.  
532 W., Levis, S., Lawrence, D. M., Kluzek, E., Lindsay, K., and Thornton, P. E.:  
533 Simulating the biogeochemical and biogeophysical impacts of transient land  
534 cover change and wood harvest in the Community Climate System Model  
535 (CCSM4) from 1850 to 2100, *J. Climate*, 25, 3071-3095, [10.1175/JCLI-D-11-](https://doi.org/10.1175/JCLI-D-11-00256.1)  
536 [00256.1](https://doi.org/10.1175/JCLI-D-11-00256.1), 2012.

537 Le Queré, C., Raupach, M. R., Canadell, J. G., Marland, G., Bopp, L., Ciais, P., Conway,  
538 T. J., Doney, S. C., Feely, R. A., Foster, P., Friedlingstein, P., Gurney, K. R.,  
539 Houghton, R. A., House, J. I., Huntingford, C., Levy, P. E., Lomas, M. R.,  
540 Majkut, J., Metzl, N., Ometto, J. P., Peters, G. P., Prentice, I. C., Randerson, J. T.,  
541 Running, S. W., Sarmiento, J. L., Schuster, U., Sitch, S., Takahashi, T., Viovy,  
542 N., van der Werf, G. R., and Woodward, F. I.: Trends in the sources and sinks of  
543 carbon dioxide, *Nature Geoscience*, 2, 831-836, [10.1038/ngeo689](https://doi.org/10.1038/ngeo689), 2009.



544 Lenton, T. M., and Huntingford, C.: Global terrestrial carbon storage and uncertainties in  
545 its temperature sensitivity examined with a simple model *Global Change Biol.*, 9,  
546 1333-1352, 2003.

547 Li, F., Bond-Lamberty, B., and Levis, S.: Quantifying the role of fire in the Earth system  
548 – Part 2: Impact on the net carbon balance of global terrestrial ecosystems for the  
549 20th century, *Biogeosciences*, 11, 1345-1360, 10.5194/bg-11-1345-2014, 2014.

550 Mao, J., Shi, X., Thornton, P. E., Piao, S., and Wang, X.: Causes of spring vegetation  
551 growth trends in the northern mid-high latitudes from 1982 to 2004, *Environ. Res.*  
552 *Let.*, 7, 014010, 10.1088/1748-9326/7/1/014010, 2012a.

553 Mao, J., Thornton, P. E., Shi, X., Zhao, M., and Post, W. M.: Remote sensing evaluation  
554 of CLM4 GPP for the period 2000–09, *J. Climate*, 25, 5327-5342, 10.1175/JCLI-  
555 D-11-00401.1, 2012b.

556 Meinshausen, M., Raper, S. C. B., and Wigley, T. M. L.: Emulating coupled atmosphere-  
557 ocean and carbon cycle models with a simpler model, *MAGICC6 – Part 1: Model*  
558 *description and calibration*, *Atmos. Chem. Phys.*, 11, 1417-1456, 10.5194/acp-11-  
559 1417-2011, 2011a.

560 Meinshausen, M., Wigley, T. M. L., and Raper, S. C. B.: Emulating atmosphere-ocean  
561 and carbon cycle models with a simpler model, *MAGICC6 – Part 2: Applications*,  
562 *Atmos. Chem. Phys.*, 11, 1457-1471, 10.5194/acp-11-1457-2011, 2011b.

563 Mitchell, T. D., and Jones, P. D.: An improved method of constructing a database of  
564 monthly climate observations and associated high-resolution grids, *Internat. J.*  
565 *Climat.*, 25, 693-712, 2005.

566 Monfreda, C., Ramankutty, N., and Hertel, T.: Global agricultural land use data for

567 climate change analysis, in: Economic Analysis of Land Use in Global Climate  
568 Change Policy, edited by: Hertel, T., Rose, S. K., and Tol, R., Routledge, New  
569 York, 368, 2009.

570 Nobre, C. A., Sellers, P. J., and Shukla, J.: Amazonian deforestation and regional climate  
571 change, *J. Climate*, 4, 957-988, 1991.

572 Norby, R. J., Warren, J. M., Iversen, C. M., Medlyn, B. E., and McMurtrie, R. E.: CO2  
573 enhancement of forest productivity constrained by limited nitrogen availability,  
574 *Proc. Nat. Acad. Sci.*, 107, 19368-19373, [10.1073/pnas.1006463107](https://doi.org/10.1073/pnas.1006463107), 2010.

575 Odum, E. P.: The strategy of ecosystem development, *Science*, 164, 262-270,  
576 [10.1126/science.164.3877.262](https://doi.org/10.1126/science.164.3877.262), 1969.

577 Oleson, K. W., Niu, G.-Y., Yang, Z.-L., Lawrence, D. M., Thornton, P. E., Lawrence, P.  
578 J., Stöckli, R., Dickinson, R. E., Bonan, G. B., Levis, S., Dai, A., and Qian, T.:  
579 Improvements to the Community Land Model and their impact on the  
580 hydrological cycle, *J. Geophys. Res.-Atmos.*, 113, G01021,  
581 [10.1029/2007JG000563](https://doi.org/10.1029/2007JG000563), 2008.

582 Oleson, K. W., Lawrence, D. M., Bonan, G. B., Flanner, M. G., Kluzek, E., Lawrence, P.  
583 J., Levis, S., Swenson, S. C., Thornton, P. E., Dai, A., Decker, M., Dickinson, R.  
584 E., Feddema, J. J., Heald, C. L., Hoffman, F. M., Lamarque, J. F., Mahowald, N.  
585 M., Niu, G.-Y., Qian, T., Randerson, J. T., Running, S. W., Sakaguchi, K., Slater,  
586 A. G., Stöckli, R., Wang, A., Yang, Z.-L., Zeng, X., and Zeng, X.: Technical  
587 Description of version 4.0 of the Community Land Model (CLM), National  
588 Center for Atmospheric Research, Boulder, 257, 2010.

589 Pechony, O., and Shindell, D. T.: Driving forces of global wildfires over the past

590 millennium and the forthcoming century, *Proc. Nat. Acad. Sci.*, 107, 19167-  
591 19170, 10.1073/pnas.1003669107, 2010.

592 Pongratz, J., Reick, C. H., Raddatz, T. J., and Claussen, M.: Effects of anthropogenic  
593 land cover change on the carbon cycle of the last millennium, *Glob. Biogeochem.*  
594 *Cycles*, 23, GB4001, 10.1029/2009GB003488., 2009.

595 Randerson, J. T., Hoffman, F. M., Thornton, P. E., Mahowald, N. M., Lindsay, K., Lee,  
596 Y.-H., Nevison, C. D., Doney, S. C., Bonan, G. B., Stöckli, R., Covey, C.,  
597 Running, S. W., and Fung, I. Y.: Systematic assessment of terrestrial  
598 biogeochemistry in coupled climate–carbon models, *Global Change Biol.*, 15,  
599 2462-2484, 10.1111/j.1365-2486.2009.01912.x, 2009.

600 Running, S. W., and Hunt, R. E.: Generalization of a forest ecosystem process model for  
601 other biomes, BIOME-BGC, and an application for global-scale models, in:  
602 *Scaling Physiologic Processes: Leaf to Globe*, edited by: Ehleringer, J. R., and  
603 Field, C. B., Academic Press, San Diego, CA, 141-158, 1993.

604 Shi, X., Mao, J., Thornton, P. E., Hoffman, F. M., and Post, W. M.: The impact of  
605 climate, CO<sub>2</sub>, nitrogen deposition and land use change on simulated contemporary  
606 global river flow, *Geophys. Res. Lett.*, 38, L08704, 10.1029/2011GL046773,  
607 2011.

608 Shi, X., Mao, J., Thornton, P. E., and Huang, M.: Spatiotemporal patterns of  
609 evapotranspiration in response to multiple environmental factors simulated by the  
610 Community Land Model, *Environ. Res. Lett.*, 8, 024012, 10.1088/1748-  
611 9326/8/2/024012, 2013.

612 Taylor, K. E., Stouffer, R. J., and Meehl, G. A.: An overview of CMIP5 and the

613 experiment design, *Bulletin of the American Meteorological Society*, 93, 485-  
614 498, [10.1175/BAMS-D-11-00094.1](https://doi.org/10.1175/BAMS-D-11-00094.1), 2012.

615 Thomson, A. M., Calvin, K. V., Chini, L., Hurtt, G. C., Edmonds, J. A., Bond-Lamberty,  
616 B., Frohking, S. E., Wise, M., and Janetos, A. C.: Climate mitigation and the  
617 future of tropical landscapes, *Proc. Nat. Acad. Sci.*, 107, 19633-19638,  
618 [10.1073/pnas.0910467107](https://doi.org/10.1073/pnas.0910467107), 2010.

619 Thornton, P. E., Law, B. E., Gholz, H. L., Clark, K. L., Falge, E., Ellsworth, D. S.,  
620 Goldstein, A. H., Monson, R. K., Hollinger, D. Y., Falk, M., Chen, J., and Sparks,  
621 J. P.: Modeling and measuring the effects of disturbance history and climate on  
622 carbon and water budgets in evergreen needleleaf forests, *Agric. Forest Meteorol.*,  
623 113, 185-222, [10.1016/S0168-1923\(02\)00108-9](https://doi.org/10.1016/S0168-1923(02)00108-9), 2002.

624 Thornton, P. E., Lamarque, J.-F., Rosenbloom, N. A., and Mahowald, N. M.: Influence of  
625 carbon-nitrogen cycle coupling on land model response to CO<sub>2</sub> fertilization and  
626 climate variability, *Glob. Biogeochem. Cycles*, 21, Art. No. GB4018,  
627 [10.1029/2006GB002868](https://doi.org/10.1029/2006GB002868), 2007.

628 Todd-Brown, K. E. O., Randerson, J. T., Hopkins, F. M., Arora, V., Hajima, T., Jones, C.  
629 D., Shevliakova, E., Tjiputra, J., Volodin, E. M., Wu, T., Zhang, Q., and Allison,  
630 S. D.: Changes in soil organic carbon storage predicted by Earth system models  
631 during the 21st century, *Biogeosciences*, 11, 2341-2356, [10.5194/bgd-10-18969-](https://doi.org/10.5194/bgd-10-18969-2013)  
632 2013, 2014.

633 van Vuuren, D. P., Bayer, L. B., Chuwah, C., Ganzeveld, L., Hazeleger, W., van den  
634 Hurk, B. J. J. M., van Noije, T., O'Neill, B. C., and Strengers, B. J.: A  
635 comprehensive view on climate change: coupling of earth system and integrated

636 assessment models, Environ. Res. Lett., 7, 024012, 10.1088/1748-  
637 9326/7/2/024012, 2012.

638 Wise, M., Calvin, K. V., Thomson, A. M., Clarke, L. E., Bond-Lamberty, B., Sands, R.  
639 D., Smith, S. J., Janetos, A. C., and Edmonds, J. A.: Implications of limiting CO<sub>2</sub>  
640 concentrations for land use and energy, Science, 324, 1183-1186,  
641 [10.1126/science.1168475](https://doi.org/10.1126/science.1168475), 2009.

642 Wise, M., and Calvin, K. V.: GCAM 3.0 Agriculture and Land Use: Technical  
643 Description of Modeling Approach, Pacific Northwest National Laboratory  
644 PNNL-20971  
645 ([https://wiki.umd.edu/gcam/images/8/87/GCAM3AGTechDescript12\\_5\\_11.pdf](https://wiki.umd.edu/gcam/images/8/87/GCAM3AGTechDescript12_5_11.pdf)),  
646 2010.

647 Wise, M., Calvin, K. V., Kyle, G. P., Luckow, P., and Edmonds, J. A.: Economic and  
648 physical modeling of land use in GCAM 3.0 and an application to agricultural  
649 productivity, land, and terrestrial carbon, Climate Change Economics, 5,  
650 1450003, 10.1142/S2010007814500031, 2014.

651

652

653 **Table 1.** Summary of simulations performed.

Name	Type	Purpose
S1	Uncoupled CLM, 1850-2010, constant (1901-1920) climate	Control for S2, S3, S4
S2	S1 + changing CO <sub>2</sub>	Single-factor experiments quantifying how
S3	S1 + changing N deposition	CO <sub>2</sub> , N deposition, and LUC affect
S4	S1 + changing LUC	potential proxy variables
E1	Uncoupled CLM, constant (2005-2009) climate	Equilibrium biomass simulations quantifying how initial NPP predicts final vegetation C
E2	Uncoupled CLM, constant (2090-2094) climate	Equilibrium biomass simulation quantifying how climate-driven changes in NPP predict changes in vegetation C
M1	Idealized Monte Carlo	Assess error that could be introduced to climate effects scalars by increasing amount of LUC.

654

655

656 **Table 2.** Slope (yr), adjusted R<sup>2</sup> value, and number of grid cells for the relationship  
657 between change in NPP in response to a climate change signal and resulting change in  
658 equilibrium biomass (simulations E1 and E2 in **Table 1**). Excluding PFTs whose  
659 cumulative carbon loss from fires exceeds 8 Mg C ha<sup>-1</sup> over 150 years generally  
660 improved the R<sup>2</sup> values and increased the slopes (data not shown).

PFT	Name	Slope	R <sup>2</sup>	Count
1	needleleaf_evergreen_temperate_tree	20.4	0.52	3500
2	needleleaf_evergreen_boreal_tree	20.5	0.68	5136
3	needleleaf_deciduous_boreal_tree	24.9	0.92	1643
4	broadleaf_evergreen_tropical_tree	18.0	0.35	2609
5	broadleaf_evergreen_temperate_tree	20.9	0.40	1702
6	broadleaf_deciduous_tropical_tree	25.2	0.56	3909
7	broadleaf_deciduous_temperate_tree	21.9	0.49	3966
8	broadleaf_deciduous_boreal_tree	23.6	0.64	5311
	<i>All trees</i>	<i>21.5</i>	<i>0.51</i>	<i>27776</i>
9	broadleaf_evergreen_shrub	1.9	0.06	299
10	broadleaf_deciduous_temperate_shrub	5.8	0.45	3336
11	broadleaf_deciduous_boreal_shrub	6.5	0.60	5979
	<i>All shrubs</i>	<i>6.0</i>	<i>0.50</i>	<i>9614</i>
12	c3_arctic_grass	1.8	0.30	6417
13	c3_non-arctic_grass	2.4	0.38	8061
14	c4_grass	1.1	0.19	5436
	<i>All grasses</i>	<i>1.6</i>	<i>0.28</i>	<i>19914</i>

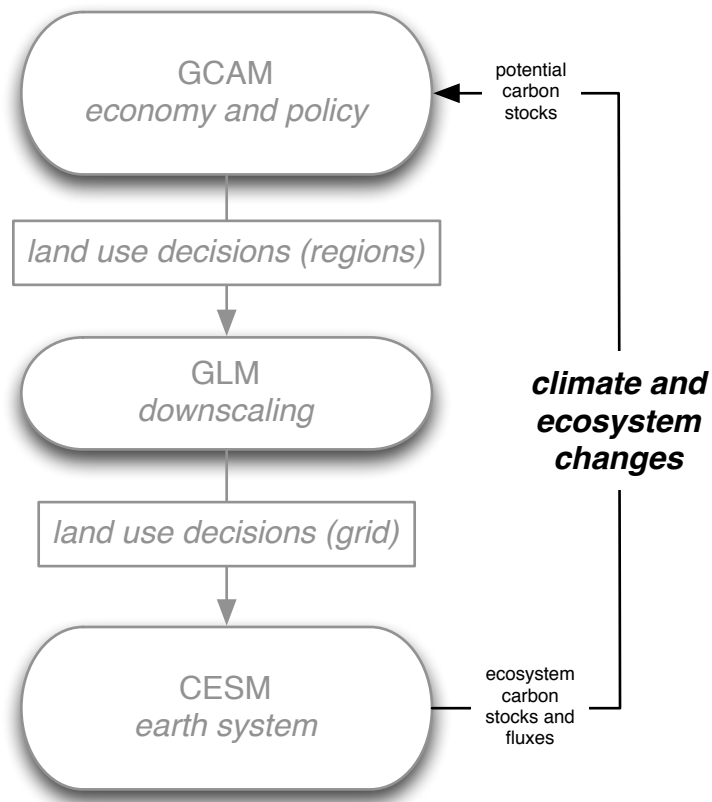
15	crop	1.7	0.19	9142
----	------	-----	------	------

661

662



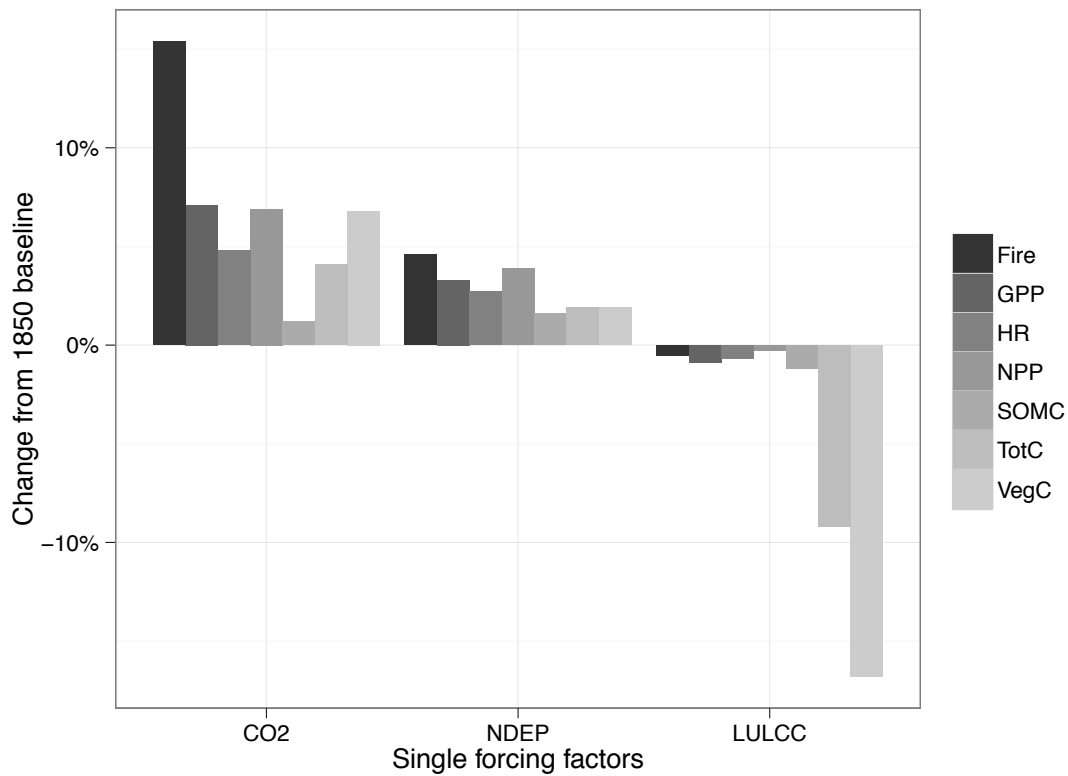
663 **Figure 1.** High-level overview of the iESM (integrated earth system model) system; a  
664 more detailed schematic is presented by Di Vittorio et al (2014). Oval boxes represent  
665 models, and arrows show data flows. This paper focuses on the information flow between  
666 CLM (part of CESM) and GCAM, in bold.



667

668

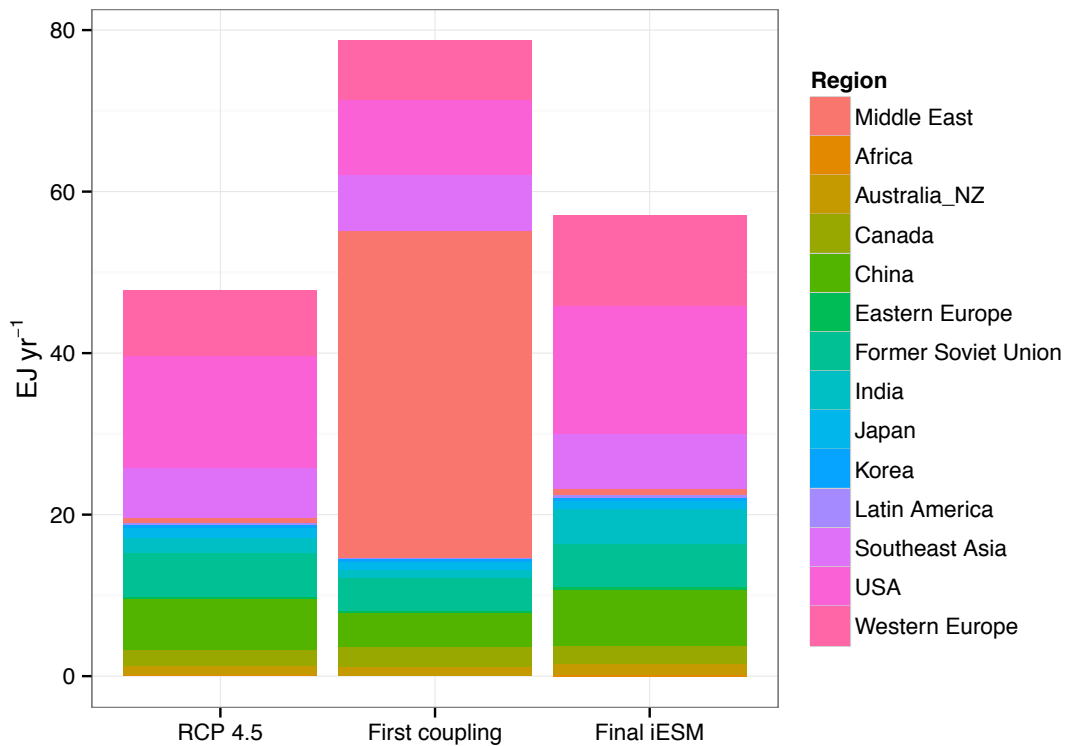
669 **Figure 2.** Response of Community Land Model outputs to changes in atmospheric CO<sub>2</sub>  
 670 (simulation S2), nitrogen deposition (NDEP, simulation S3), and land-use/land cover  
 671 change (LULLC, simulation S4; cf. **Table 1**). Outputs shown are all relative to an 1850  
 672 baseline, as described in the text, and include fire emissions (Fire), terrestrial gross  
 673 primary production (GPP), heterotrophic respiration (HR), net primary production (NPP),  
 674 carbon in soil organic matter (SOMC), total ecosystem carbon (TotC), and total  
 675 vegetation carbon (VegC).



676

677

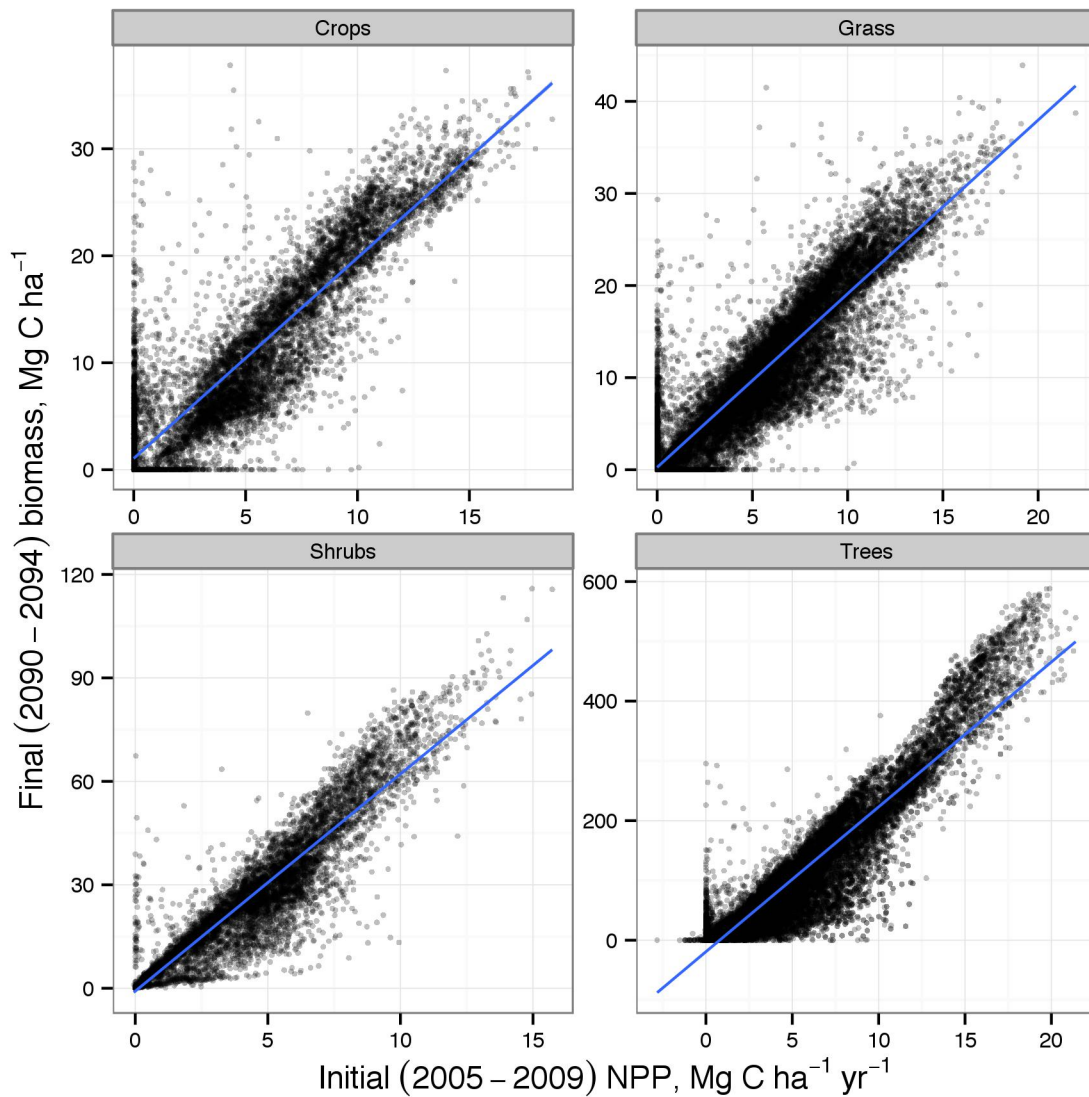
678 **Figure 3.** GCAM model output (energy derived from bioenergy by region of the world)  
 679 in three model runs, the RCP4.5 control, a coupled CLM-GCAM run using carbon stocks  
 680 as a coupling mechanism, and a run using the final coupling described in the text. In the  
 681 second case the model diverged sharply and unrealistically from the RCP4.5 control,  
 682 because the vulnerability of C stock data to disturbance effects triggered a feedback loop  
 683 in GCAM. The final run, incorporating the coupling and outlier-exclusion mechanisms  
 684 described in the text, showed no such divergence. Data are from model year 2065, when  
 685 the second run was stopped.



686

687

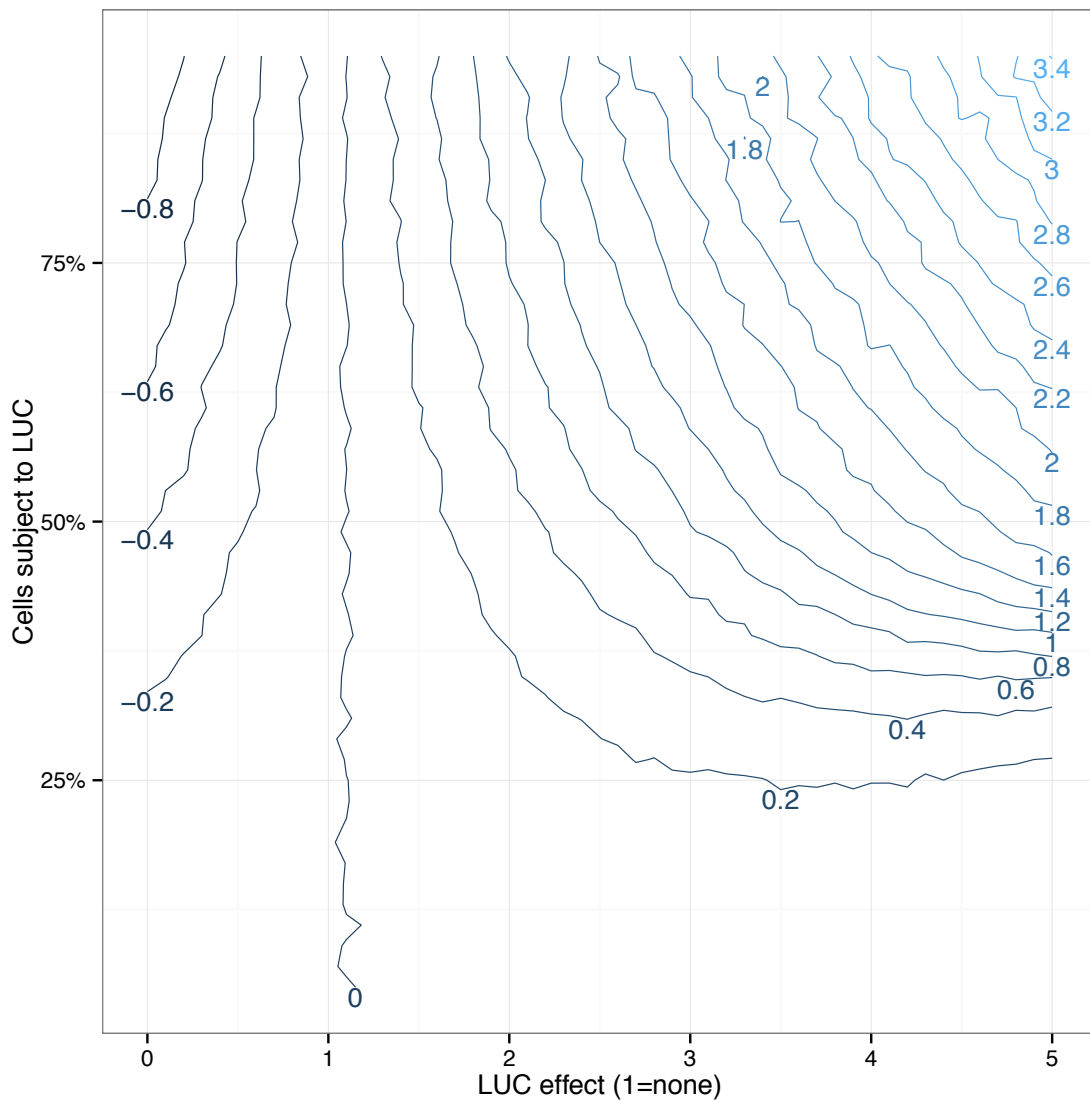
688 **Figure 4.** Relationship between net primary production (NPP, 2005-2009) to biomass  
689 (2090-2094) in CLM for crops, grasses, shrubs, and trees; cf. **Table 2**. Lines show best-  
690 fit linear regressions. Results are from the E1 and E2 simulations in **Table 1**.



691

692

693 **Figure 5.** Monte Carlo simulation M1 (cf. **Table 1**) examining if an outlier test can  
 694 distinguish between artificial climate and land use change (LUC) signals. Contour lines  
 695 (every 20%) show error between the inferred climate change signal and the known signal  
 696 as increasing numbers of cells (y axis) are perturbed by LUC with increasing effect (x  
 697 axis). The effect (i.e., intensity) is shown as the ratio of perturbed cells' equilibrium C to  
 698 that of unperturbed cells: a doubling (e.g. transitioning from crop to young forest) is an  
 699 effect of 2.0, a halving as 0.5, etc.



700